Journal of Solid State Chemistry 334 (2024) 124693

Contents lists available at ScienceDirect

Journal of Solid State Chemistry

journal homepage: www.elsevier.com/locate/jssc

The phases formed in Sn/Co thin bilayer upon heating

Leonid Eremin [a], Alexey Matsynin [a,b], Yurii Balashov [a,*], Victor Myagkov [a], Victor Zhigalov [a], Lydmila Bykova [a], Sergey Komogortsev [a,b]

[a] Kirensky Institute of Physics, Federal Research Center KSC SB RAS, Krasnoyarsk, 660036, Russia
[b] Applied Physics Department, Reshetnev Siberian State University of Science and Technology, 660037, Krasnoyarsk, Russia

ARTICLE INFO

Keywords:
Thin films
Solid-state chemistry
Metallic bilayer
Annealing

ABSTRACT

The structure and phases formed in Sn/Co thin films are interesting both from the solid-state chemistry point of view and due to applications of such a metallic bilayer. The phases forming in thin films Sn/Co obtained by thermal vacuum evaporation on two different substrates SiO_2 and MgO(100) at different annealing temperatures have been studied. Annealing above 110°C results in intermetallics formation in the films. The hcp-cobalt is grown in the films on SiO_2 substrate, and the fcc-Co is observed on MgO(100) substrate. It is found that the stable α-Co_3Sn_2 intermetallic is formed at higher annealing temperature in film on MgO(100) substrate. We show that transformations related to mass transfer in the Sn/Co bilayers were up to 500°C and were finished upon reaching the thermodynamically equilibrium phase composition at this temperature.

1. Introduction

An interest in studying diffusion and solid-state reactions in thin films containing several different layers is caused by the problem of stability of multilayer film systems in nanoelectronics. An intensive developing knowledge on the fundamentals of solid-state chemical transformations is also raised the interest in experimental studies in the field [1–7]. Cobalt and tin-based cobalt alloys are considered and investigated because of their applicability as lead-free solders [8–11]. The Sn–Co alloys and Sn/Co contacts are also used in lithium-ion battery electrodes [12,13]. The phase formation at the Sn/Co interface has been studied in a number of works [9–11]. Most of the works on mutual diffusion or formation of intermetallics were performed on layers with thickness of 10 μm or more [9–11,14]. However, a miniaturization of functional elements down to the nanometer scale requires studies on layers with thicknesses from units to tens of nanometers [15,16]. But in this case, one can expect peculiarities both in the diffusion and in the phase formation at the interface. The great surface role in nanolayers leads to a substrate importance. In this work the transformations in about 100 nm thick bilayers prepared on different substrates are studied.

The study was carried out on bilayer Sn/Co structures with the elements ratio of about 1/3, deposited on MgO(100) and glass, at the different annealing temperatures up to 500°C. Note that there are no works on this bilayer where annealing temperatures exceed 350°C [9–11]. In this work, we show that transformations related to mass transfer in the Sn/Co bilayers were up to 500°C and were finished upon reaching the thermodynamically equilibrium phase composition at this temperature.

2. Materials and methods

The bilayers Sn/Co were synthesized by thermal evaporation and then annealed. The first bilayer Sn/Co films was deposited by a sequential thermal evaporation onto glass and monocrystalline MgO (100) substrates at a vacuum of 10^{-6} Torr. The cobalt layer was deposited to substrate heated up to 300°C using the electron-beam-induced deposition from (Mo + Al_2O_3) – crucible. After deposition, the cobalt layer on MgO was immediately annealed in the chamber at 600°C for 2 h to ensure high quality of epitaxy. Then the Sn layer was deposited onto the Co layer at the room temperature using a molybdenum crucible.

After that the bilayers were isothermally annealed in a vacuum of 10^{-6} Torr. The annealing was at the temperatures 100, 200, 300, 400, 500°C for 90 min. The first annealing was at T = 100 °C, then the same sample was annealed at T = 200 °C, T = 300 °C etc. The X-ray diffraction and magnetic studies were caried out at room temperature after each annealing step. According to an X-ray fluorescent analysis, the Co and Sn contents were 76 ± 2 and 24 ± 2 at.%, respectively (the corresponding Co and Sn layers thicknesses are 85 nm and 60 nm). The identification of the phases was carried out by X-ray diffraction analysis using the DRON-

* Corresponding author.
E-mail address: y.balashov@yandex.ru (Y. Balashov).

https://doi.org/10.1016/j.jssc.2024.124693
Received 19 December 2023; Received in revised form 21 March 2024; Accepted 25 March 2024
Available online 27 March 2024

4-07 diffractometer (XRD, CuKα radiation). Measurements of magnetic properties (anisotropy constant – K_1 and a saturation magnetization M_S) were carried out using a torsion magnetometer. The studied film sample is suspended on a vertical torsion thread and placed in an external magnetic field. After that, the rotation angle of the sample is measured at different field orientations relative to the sample. The measured torque provides information on the magnetization and anisotropy constant [17]. The applied field range was 0 ÷ 12 kOe.

The temperature behavior of the electrical resistance of the samples was studied by the four-probe method in a vacuum of 10^{-6} Torr from the room temperature to 520°C with the heating rate 4°C/min.

3. Results

The phases formed in the films at the different annealing temperatures were identified using the X-ray patterns (see Fig. 1) and provided in Table 1. Fig. 1 shows that the films consist only of pure Co and β-Sn (tetragonal crystal structure; space group –I41/amd) elements after annealing at 100 °C of both samples on SiO_2 and MgO(100) substrates, i.e., no solid state reactions are observed. However, it is revealed that the structure of cobalt grown on different substrates is different: the α-Co (cobalt with the hcp structure) was formed on the SiO_2 substrate, while the β-Co (cobalt with the fcc structure) was formed on the MgO(100) substrate. Moreover, it is seen from Fig. 1b that the structure of β-Sn and Co layers grown on the MgO(100) is related to the substrate crystallographic orientation as β-Sn(100) || β-Co(100) || MgO(100), since the XRD peaks in Fig. 1b are only from the (200)β-Co and (200)β-Sn and (400)β-Sn planes. This means epitaxy in this system [18,19]. Note that the α-Co phase is stable at room temperature. The growing of the metastable β-phase on the MgO(100) substrate is mainly caused by both the epitaxy of the cobalt layer to the substrate and the subsequent annealing at the 600 °C (see section "2 Methods and materials"). At the 600 °C, the β-phase of cobalt is stable. During annealing at 600 °C (before the sputtering of the Sn), both the β-Co and its epitaxial coupling with the MgO(100) substrate appear to be formed. The transition to β-Co → α-Co is prevented by that epitaxial coupling at the subsequent cooling.

Table 1
Phases formed in the Sn/Co bilayer as the annealing temperature increases. The first row corresponds to the as-prepared bilayer Sn/Co. The phases formed during annealing at different temperatures are shown below.

Amorphous substrate SiO_2		Single-crystalline substrate MgO(100)
α-Co + Sn		β-Co + Sn
	200 °C	
α-Co + Sn + α-$CoSn_3$		β-Co + Sn + α-$CoSn_3$
	300 °C	
α-Co + $CoSn_2$ + CoSn + α-$CoSn_3$		β-Co + $CoSn_2$ + CoSn + α-$CoSn_3$
	400 °C	
α-Co + α-Co_3Sn_2 + CoSn		β-Co + $CoSn_2$ + CoSn
	500 °C	
α-Co + α-Co_3Sn_2		β-Co + α-Co_3Sn_2

The Co layer in the samples obtained on the amorphous substrate SiO_2 was not exposed to such annealing. Moreover, the growing of a cobalt on such substrate is not epitaxial, so the formation of a stable α-Co is understandable in this case. After annealing at 200 °C and above, the films contain Co–Sn intermetallics. The reaction between Co and Sn starts with the formation of the α-$CoSn_3$, within the temperature range of 100 °C < T < 200 °C on both types of the substrates. The first appearance of the α-$CoSn_3$ phase is following to a First phase rule. According to this rule [20,21]: the first phase formed at the interface between the film reagents is the phase which is coincided with the lowest temperature of structural-phase transformation (order-disorder, martensitic, spinodal decomposition, eutectic reaction, etc.) in the equilibrium diagram. The lowest temperature of eutectic transformation is T = 231 °C for the α-$CoSn_3$ – Sn pair according to the Co–Sn phase diagram [22]. Thus, the fact that the solid-state reaction at the Sn/Co interface starts with the α-$CoSn_3$ phase formation is followed to First phase rule.

However, the binary system Sn–Co with the component ratio Sn:Co = 1:3 (our case) would have the phase composition Co + α-Co_3Sn_2 in the thermodynamic equilibrium [22,23]. The formation of this phase

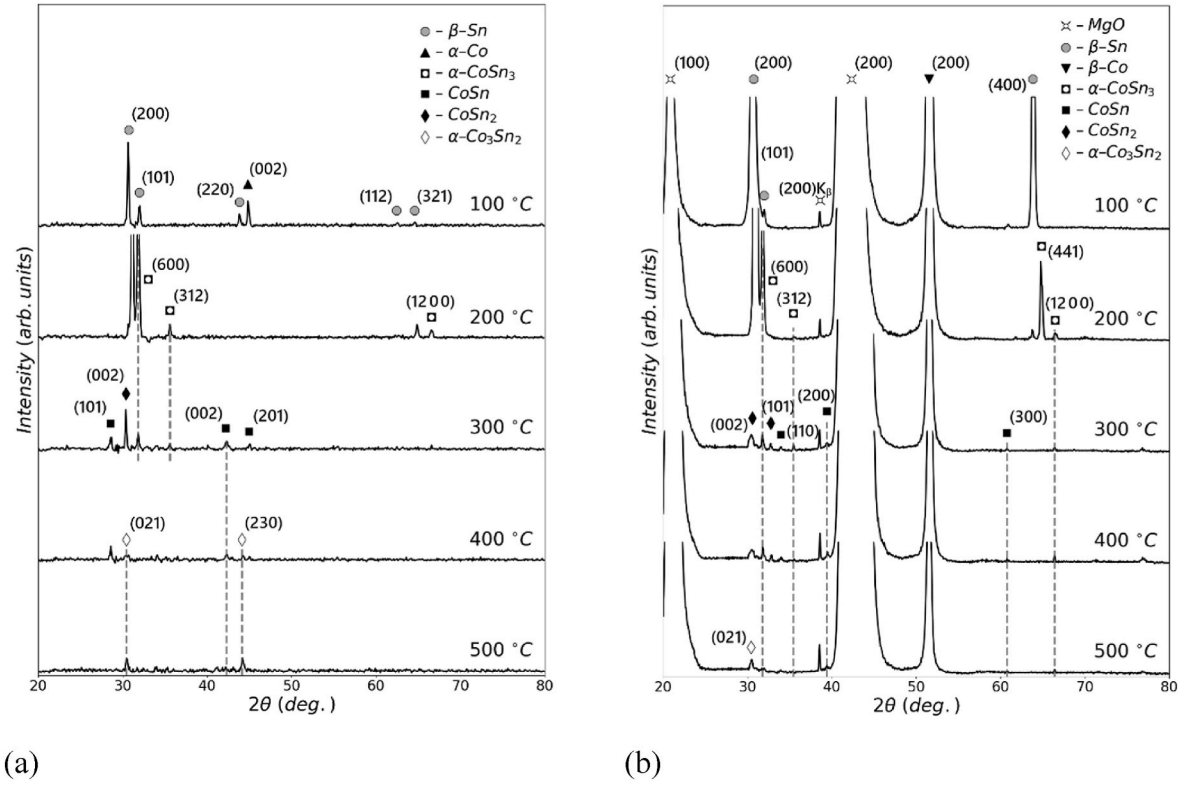

Fig. 1. X-ray patterns of Sn/Co films: (a) on SiO_2 substrate; (b) on MgO(100) substrate.

composition is observed after annealing at 500 °C. The leverage rule evaluation provides an amount of a cobalt in the thermodynamically equilibrium samples would be 40%. Since the intermetallics observed in this work have no or negligible magnetization [24–26], compared to that of pure cobalt (1400 Gs), one can estimate the fraction of cobalt in the sample by the value of the film magnetization. Fig. 2 shows how the fraction of a Co estimated in this way decreases as the annealing temperature increases (see also the discussion for this figure). At the T_{an} = 500 °C, the Co fraction is 0.38 of the initial amounts of pure cobalt (38%). Since this perfectly close to the cobalt fraction estimated using the leverage rule, it can be concluded that the annealing at 500 °C is the final point of the solid-state transformations, at which the system is reached the thermodynamic equilibrium.

The equilibrium intermetallic compound α-Co_3Sn_2 is formed on the MgO(100) substrate at a higher annealing temperature. This can be explained by the greater perfection of film-surface interfaces in samples on the single-crystalline MgO(100) substrate compared to that obtained on the amorphous SiO_2 substrate. The nucleation of a new phase by the heterogeneous mechanism should be stimulated by the surface roughness. Since the roughness of the single-crystalline MgO substrate would be lower the conditions for the nucleation are suppressed. Thus, the temperature of new phase formation is expected to be higher in this case.

In the method [17], which is used for the estimation of the values of M_s and K_1, the variation of the torque of the film sample in different fields is used. Ultimately, the values of $M_S{\cdot}V$ and $K_1{\cdot}V$ are independently estimated by this method, where V is the volume of the magnetic layer, M_S and K_1 are its magnetization and magnetic anisotropy constant, respectively. Since in this paper only the Co layer have spontaneous magnetization, the measured values of $M_S{\cdot}V$ and $K_1{\cdot}V$ are determined by the Co volume only. So, by the changing the values of $M_S{\cdot}V$ and $K_1{\cdot}V$ the volume fraction of Co in the film can be estimated as:

$$M_s \cdot V_{Co}/M_s{\cdot}V_{Co}^{asprepared} = V_{Co}/V_{Co}^{asprepared} = \nu_{Co}, \quad (1)$$

or

$$K_1 \cdot V_{Co}/K_1{\cdot}V_{Co}^{asprepared} = V_{Co}/V_{Co}^{asprepared} = \nu_{Co} \quad (2)$$

From this estimation (Fig. 2) the Co volume fraction decreases as the annealing temperature increase, which one can expect in view of the data of Table 1. As mentioned above, this estimation allows us to conclude that the thermodynamic equilibrium of the given system, predicted by the Co–Sn phase diagram, is reached at the annealing of 500 °C. The sequential emerging of the intermetallics $CoSn_3$, $CoSn_2$, CoSn, Co_3Sn_2 is observed, from the first reaction stage (with forming the $CoSn_3$) to the final that (when existing the Co_3Sn_2), which corresponds to a gradual increase in the amount of cobalt in the observed compounds.

The temperature behavior of the electrical resistance of Sn/Co film (Fig. 3) with temperature increase indicate the irreversible processes

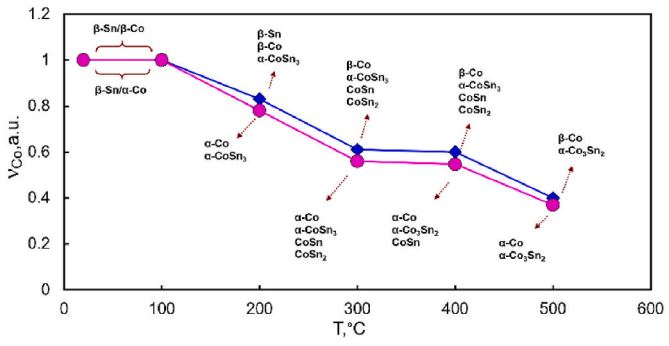

Fig. 2. Volume fraction of Co estimated from torque measurements in a magnetic field: diamond symbol is estimation using effective anisotropy constant and circle is estimation using the magnetization.

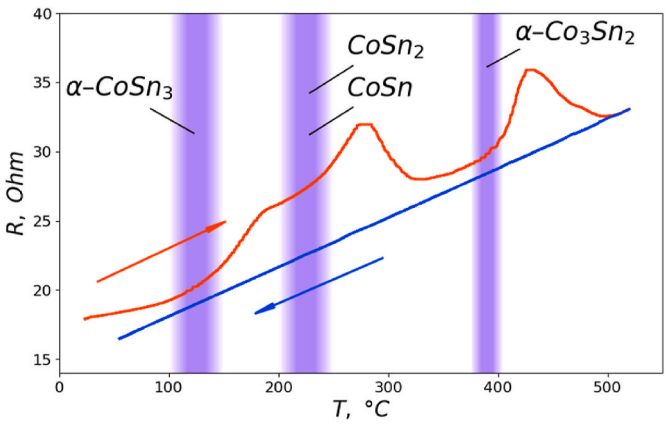

Fig. 3. Temperature behavior of electrical resistance in Sn/Co film.

(solid-state reactions) starting from 110 to 140 °C. This indicates the start of phase transformations. The indications and the temperatures of the starting transformations are related with significant deviations from the linear reversible resistance growth. For example, at the temperature range of 110–140 °C the resistance starts to increase nonlinearly and irreversibly. It seems reasonable to associate this with the beginning of the α-$CoSn_3$ formation. The temperature behavior of the electrical resistivity allows us to refine the temperatures of the compound formations in the film. The rough estimate of such temperatures was done from the XRD analysis (see Fig. 1 and Table 1). The temperatures of the start of each phase formation are plotted as the color vertical bands with blurred edges, which are associated with the absence of clear boundaries of these bands in Fig. 3.

The intensive irreversible decrease of the resistance is observed at the 280 and 430 °C. This can be attributed to two mechanisms: 1) the transition from island structure of the CoSn (at 280 °C) and α-Co_3Sn_2 (at 430 °C) phases to continuous layers; 2) the changing effective film thickness during the solid-state reaction. Reduction of resistance by the first mechanism is assumed to be abrupt because the electron dissipation in the multilayer system is lower than in the granular system, which would have more dissipation centers.

The second mechanism is that the Sn layer thickness of the as-prepared sample is very inhomogeneous. At the initial reaction stages, the electrical resistance of the layer is sensitive to the minimal thickness. As the intermetallics are formed, the tin layer is uniformly distributed over the entire film volume. As a result, its thickness is homogenized and the total effective thickness is increased [27], that would also lead to the electric resistance decrease. During the film cooling from the maximum temperature (520 °C), the behavior of the film electrical resistance exhibits a linear and reversible decrease. This implies that there are no solid-state transformations and this is in accordance with the idea of the reaching the thermodynamic equilibrium of the alloy above 500 °C discussed above.

Let's discuss the observed sequence of emerging phases in terms of a free energy. The data on the temperature behavior of the free energy of the compounds in the Co–Sn system from Refs. [22,28–33] are summarized in Fig. 4.

Since the data of various works concerning the same compounds vary significantly and are characterized by certain experimental errors, the energy related to one phase in Fig. 4 is represented not by a line, but by a blurred bond. Note that the observed sequence of emerging phases is not contrary to Fig. 4. It should be expected that the sequence of emerging reaction products, as the annealing temperature increases, should be in accordance with the energy of the system decrease gradually ($\Delta G_0 > \Delta G_1 > \ldots > \Delta G_n$) starting from the initial most nonequilibrium state (Co + Sn). For example, the annealing at 200 °C for 40 min leads to the formation of the highest energy (closest to the most nonequilibrium state – Co + Sn) phase α-$CoSn_3$ (see Table 1). Further, the annealing at

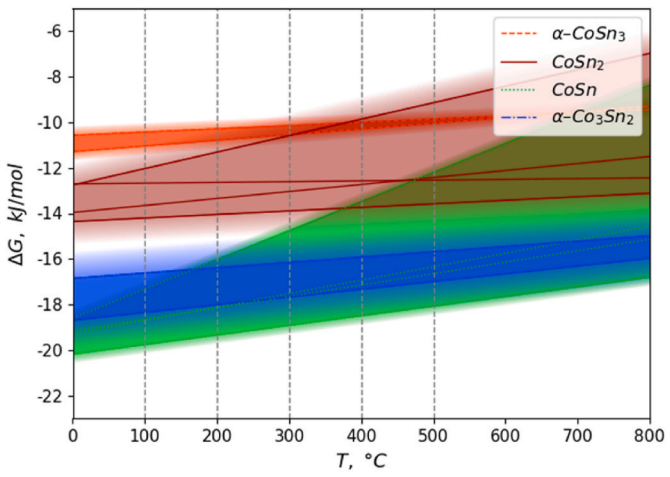

Fig. 4. The temperature behavior of the free energy ΔG of the compounds in the Co–Sn system according data from refs [22,28–33].

300 °C additionally leads to the formation of phases $CoSo_2$ and CoSn characterized by a lower energy, i.e. the average energy of the system ($CoSo_2$ + CoSn + α-$CoSn_3$) is below the energy of α-$CoSn_3$. After the annealing at 400 °C, the system (α-Co_3Sn_2 + CoSn) is formed, the average energy of which is lower than the energy of the previous set of phases. Finally, the annealing at 500 °C results in the single intermetallic compound α-Co_3Sn_2. According to Fig. 4, the center of the α-Co_3Sn_2 band is slightly lower than the center of the CoSn band, so the observation of α-Co_3Sn_2 is not contrary to Fig. 4, either.

4. Conclusions

The phase formation of in Sn/Co thin films on SiO_2 and MgO(001) substrates at different annealing temperatures obtained by thermal evaporation in a high vacuum has been studied using X-ray diffraction analysis and torque measurements in a magnetic field. For Sn/Co bilayer structures with an element ratio about 1/3 (thicknesses of 60 and 85 nm, respectively) the temperatures and the sequence of emerging phases are established. In the bilayer on a single-crystal MgO (100) substrate the phases formed are: β-Co/Sn (200 °C)→ β-Co + Sn + α-$CoSn_3$ (300 °C)→ β-Co + $CoSn_2$ + CoSn + α-$CoSn_3$(400 °C)→ β-Co + $CoSn_2$ + CoSn (500 °C)→β-Co+α-Co_3Sn_2.

In the sample on a glass substrate the sequence of phase transformations is: α-Co/Sn (200 °C)→ α-Co + Sn + α-$CoSn_3$ (300 °C)→ α-Co + $CoSn_2$ + CoSn + α-$CoSn_3$(400 °C)→ α-Co + α-Co_3Sn_2 + CoSn (500 °C)→ α -Co+α-Co_3Sn_2. Additional study of the temperature behavior of electrical resistivity shows that the formation of intermetallics begins at 110 °C. When the film is annealed above 500 °C, the thermodynamically equilibrium phase composition is reached according to equilibrium Co–Sn phase diagram. The β-Co is formed on MgO(001) substrate and α-Co on SiO_2 substrate. It is found that the equilibrium intermetallic phase α-Co_3Sn_2 is formed on MgO(001) substrate at higher annealing temperature than on SiO_2 substrate.

Funding

The authors declare that no funds, grants, or other support were received during the preparation of this manuscript.

CRediT authorship contribution statement

Leonid Eremin: Writing – original draft, Investigation. **Alexey Matsynin:** Methodology, Investigation. **Yurii Balashov:** Writing – original draft, Visualization, Formal analysis. **Victor Myagkov:** Methodology, Conceptualization. **Victor Zhigalov:** Investigation. **Lydmila Bykova:** Investigation. **Sergey Komogortsev:** Writing – original draft, Project administration, Investigation, Formal analysis.

Declaration of competing interest

The authors declare that they have no known competing financial interests or personal relationships that could have appeared to influence the work reported in this paper.

Data availability

Data will be made available on request.

References

[1] D.P. Adams, Reactive multilayers fabricated by vapor deposition: a critical review, Thin Solid Films 576 (2015) 98–128, https://doi.org/10.1016/j.tsf.2014.09.042.
[2] Y.D. Tretyakov, Self-organization processes in the chemistry of materials, Russ. Chem. Rev. 72 (8) (2003) 651–679, https://doi.org/10.1070/RC2003v072n08ABEH000836.
[3] Y.D. Tretyakov, Development of inorganic chemistry as a fundamental for the design of new generations of functional materials, Russ. Chem. Rev. 73 (9) (2004) 831–846, https://doi.org/10.1070/RC2004v073n09ABEH000914.
[4] V. Myagkov, et al., Long-range chemical interactions in solid-state reactions: effect of an inert Ag interlayer on the formation of L1 $_0$ -FePd in epitaxial Pd(0 0 1)/Ag(0 0 1)/Fe(0 0 1) and Fe(0 0 1)/Ag(0 0 1)/Pd(0 0 1) trilayers, Phil. Mag. 94 (23) (2014) 2595–2622, https://doi.org/10.1080/14786435.2014.926037.
[5] H.K. Kannojia, P. Dixit, A review of intermetallic compound growth and void formation in electrodeposited Cu–Sn Layers for microsystems packaging, J. Mater. Sci. Mater. Electron. 32 (2021) 6742–6777, https://doi.org/10.1007/s10854-021-05412-9.
[6] S.A. Bashkirov, et al., $Cu_2ZnSn(S,Se)_4$ thin films for application in third generation solar cells, Alternative Energy Ecol. (ISJAEE) 15–18 (2016) 31–53, https://doi.org/10.15518/isjaee.2016.15-18.031-053.
[7] E.N. Sheftel, et al., FeZrN films: magnetic and mechanical properties relative to the phase-structural state, Materials 15 (1) (2021) 137, https://doi.org/10.3390/ma15010137.
[8] A. Yakymovych, et al., Enthalpy of mixing of liquid Co–Sn alloys, J. Chem. Therm. 74 (2014) 269–285, https://doi.org/10.1016/j.jct.2014.02.013.
[9] V.A. Baheti, Phase evolutions and growth kinetics in the Co–Sn system, SN Appl. Sci. 1 (2) (2019) 185, https://doi.org/10.1007/s42452-019-0207-z.
[10] C. Wang, S. Chen, Sn/Co solid/solid interfacial reactions, Intermetallics 16 (4) (2008) 524–530, https://doi.org/10.1016/j.intermet.2007.12.017.
[11] C. Wang, et al., Temperature effects on liquid-state Sn/Co interfacial reactions, Intermetallics 32 (2013) 57–63, https://doi.org/10.1016/j.intermet.2012.07.029.
[12] V. Milanova, et al., Morphology of intermetallic (Co-Sn, Ni-Sn) nanoparticles, electrochemically tested as electrodes in li-ion battery, Journal of Chem. Technol. Metall. 52 (3) (2017) 542–556.
[13] N. Tamura, et al., Mechanical stability of Sn–Co alloy anodes for lithium secondary batteries, Electrochim Acta. Elsevier 49 (12) (2004) 1949–1956, https://doi.org/10.1016/j.electacta.2003.12.024.
[14] B. Hailong, et al., Influence of Ag content on the formation and growth of intermetallic compounds in Sn–Ag–Cu solder, J. Mater. Sci. Mater. Electron. 31 (13) (2020) 10105–10112, https://doi.org/10.1007/s10854-020-03556-8.
[15] P.Y. Chia, A.S.M.A. Haseeb, Intermixing reactions in electrodeposited Cu/Sn and Cu/Ni/Sn multilayer interconnects during room temperature and high temperature aging, J. Mater. Sci. Mater. Electron. 26 (1) (2015) 294–299, https://doi.org/10.1007/s10854-014-2398-9.
[16] A.S. Komlev, et al., Magnetoresistance features at the magnetic field-induced phase transition in FeRh thin films, J. Math. Fund. Sci. 55 (1) (2023) 16–28, https://doi.org/10.5614/j.math.fund.sci.2023.55.1.2.
[17] S. Chikazumi, Epitaxial growth and magnetic properties of single-crystal films of iron, nickel, and permalloy, J. Appl. Phys. Am. Instit. Phys. 32 (3) (1961) S81–S82.
[18] Y. Nukaga, et al., Structure and magnetic properties of Co epitaxial thin films grown on MgO single-crystal substrates, IEEE Trans. Magn. 45 (6) (2009) 2519–2522, https://doi.org/10.1109/TMAG.2009.2018643.
[19] Y. Nukaga, et al., Microstructure of Co(1120) epitaxial thin films, grown on MgO (100) single-crystal substrates, J. Phys. Conf. Ser. 200 (7) (2010) 072071, https://doi.org/10.1088/1742-6596/200/7/072071.
[20] V.G. Myagkov, et al., Solid-phase reactions and the order-disorder phase transition in thin films, Tech. Phys. 46 (6) (2001) 743–748, https://doi.org/10.1134/1.1379645.
[21] V.G. Myagkov, et al., Solid-state synthesis, rotatable magnetic anisotropy and characterization of Co1-xPtx phases in 50Pt/50fccCo(001) and 32Pt/68fccCo(001) thin films, J. Alloys Compd. 861 (2021) 157938, https://doi.org/10.1016/j.jallcom.2020.157938.
[22] G.P. Vassilev, K.I. Lilova, J.C. Gachon, Calorimetric and phase diagram studies of the Co–Sn system, Intermetallics 15 (9) (2007) 1156–1162, https://doi.org/10.1016/j.intermet.2007.02.006.
[23] H. Okamoto, Co-Sn (cobalt-tin), J. Phase Equilibria Diffus. Springer Nature BV 27 (3) (2006) 308.

[24] R. Pahari, et al., Quantum phase transition and ferromagnetism in $Co_{1+x}Sn$, Phys. Rev. B 99 (18) (2019) 184438, https://doi.org/10.1103/PhysRevB.99.184438.
[25] K. Väyrynen, et al., Atomic layer deposition of intermetallic Co_3Sn_2 and Ni_3Sn_2 thin films, Adv. Mater. Interfac. 6 (3) (2019) 1801291, https://doi.org/10.1002/admi.201801291.
[26] B.C. Sales, et al., Tuning the flat bands of the kagome metal CoSn with Fe, In, or Ni doping, Phys. Rev. Mater. 5 (4) (2021) 044202, https://doi.org/10.1103/PhysRevMaterials.5.044202.
[27] YuYu Balashov, et al., Features of the course of the solid-state reactions in a Sn/Fe/Cu trilayer film system, Tech. Phys. 68 (7) (2023) 940, https://doi.org/10.61011/TP.2023.07.56642.73-23.
[28] V. Jedličková, et al., The thermodynamic assessment of the Co-Sn system, J. Phase Equilibria Diffus. 40 (2019) 21–33, https://doi.org/10.1007/s11669-018-0687-3.
[29] K. Ishida, et al., The Co-Sn (cobalt-tin) system, J. Phase Equil. 12 (1991) 88–93, https://doi.org/10.1007/BF02663681.
[30] M. Jiang, et al., A thermodynamic assessment of the Co–Sn system, Calphad 28 (2) (2004) 213–220, https://doi.org/10.1016/j.calphad.2004.08.001.
[31] L. Liu, et al., Thermodynamic assessment of the Sn-Co lead-free solder system, J. Electron. Mater. 33 (2004) 935–939, https://doi.org/10.1007/s11664-004-0019-8.
[32] K. Lilova, Thermochemical and Topological Studies of Systems Constituted by Transition Metals (Co, Ni) with Sn and Bi (Doctoral Dissertation, Université Henri Poincaré-Nancy I), 2007.
[33] B. Predel, W. Vogelbein, Bildungsenthalpien fester legierungen der binären systeme des eisens, kobalts und nickels mit germanium und zinn, Thermochim. Acta 30 (1–2) (1979) 201–215, https://doi.org/10.1016/0040-6031(79)85054-6.